Pergamon

0277-5387(94)00424-2

*Polyhedron* Vol. 14, No. 11, pp. 1495–1515, 1995

0277-5387/95 $9.50+0.00

# OXOVANADIUM(IV) AND AMINO ACIDS—VIII. L-HISTIDINE DERIVATIVES AND RELATED LIGANDS: A SPECTROSCOPIC STUDY

**J. COSTA PESSOA* and S. M. LUZ**

Centro de Química Estrutural, Instituto Superior Técnico, 1096 Lisboa, Portugal

**and**

**R. D. GILLARD***

Department of Chemistry, University of Wales, P.O. Box 912, Cardiff CF1 3TB, Wales, U.K.

(*Received* 10 *June* 1994; *accepted* 5 *October* 1994)

**Abstract**—The coordination structures of various species in aqueous solutions of oxovanadium(IV) + derivatives of L-histidine (**1**) and related ligands (3-methyl-L-histidine, 1-methyl-L-histidine, L-histidine methyl ester, L-histidinol, *N*α-acetyl-L-histidine and histamine) have been studied by investigating the pH dependence of the circular dichroism, isotropic absorption and electron spin resonance spectra, and are compared with the structures of the corresponding complexes of L-histidine. Comparison of the spectroscopic results for all systems studied indicates coordination geometries.

Knowledge of the complex equilibria of $VO^{2+}$ in the presence of amino acids is relevant in understanding its possible interaction with likely biological ligands. V—N(his) bonding has been inferred in some enzymes.[1] The design of model systems, preferably with L-histidine (L-his) as a ligand, and a better knowledge of the coordination modes of this amino acid to $VO^{2+}$ are therefore of interest.

The crystal and molecular structure of $[(CH_3)_4N][V^{IV}O(L\text{-}hisO^-)(NCS)_2]\cdot H_2O$ has been determined by X-ray diffraction.[2] L-his functions as a tridentate chelate with the carboxylate group coordinating *trans* to the vanadyl bond, the V—N(imidazole) bond length (2.081 Å) being somewhat shorter than the V—N(amino) bond length (2.132 Å). The crystal and molecular structure of an oxo-bridged dinuclear $V^{III}$ complex $[V^{III}_2(L\text{-}hisO^-)_4(\mu\text{-}O)]\cdot 2H_2O$ have also been reported.[3]

We recently reported[4,5] studies on the L-histidine + $VO^{2+}$ system in aqueous solution by combining the results of potentiometric and spectroscopic techniques. The present objective is to clarify the structures of species formed in this system. This was done by a comparison of the pH dependence of the visible circular dichroism, visible isotropic absorption and electron spin resonance (ESR) spectra obtained for the L-histidine (**1**) + $VO^{2+}$ system with the corresponding spectra for several L-histidine derivatives and related ligands: 3-methyl-L-histidine (**2**), 1-methyl-L-histidine (**3**), L-histidine methyl ester (**4**), L-histidinol (**5**), *N*α-acetyl-L-histidine (**6**) and histamine (**7**).

For the formulations $(VO)_p(\text{ligand})_qH_r$ we normally use the abbreviation $M_pL_qH_r$. All species will be compared with the corresponding stoichiometries for the L-histidine + $VO^{2+}$ system which are defined according to the reaction ($L^- = \mathbf{1}$):

$$pM^{2+} + qL^- + rH^+ \rightleftharpoons M_pL_qH_r. \quad (1)$$

* Authors to whom correspondence should be addressed.

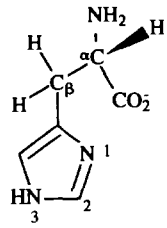

(1)

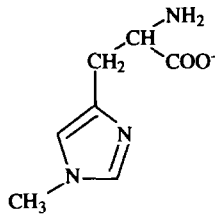

(2)

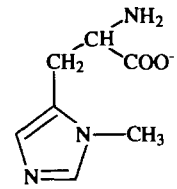

(3)

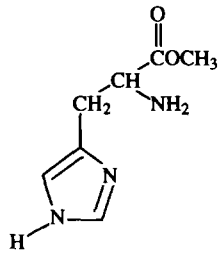

(4)

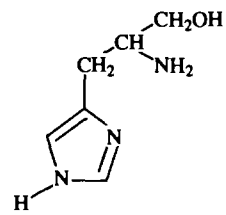

(5)

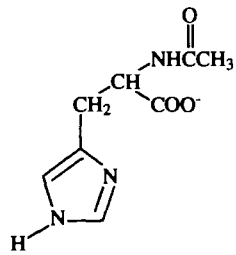

(6)

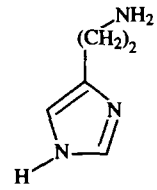

(7)

## EXPERIMENTAL

All solutions were prepared in an inert atmosphere (high purity $N_2$ passed through soda lime and glass wool). All measurements were made at 25°C with solutions containing 2.25 M $NaNO_3$. $VO^{2+}$ and NaOH solutions were prepared and standardized as described in Part I.[6] Other reagents are commercially available and were used without further purification.

### *Spectroscopic measurements*

Visible spectra were recorded with a Perkin–Elmer lambda 9 spectrophotometer and circular

dichroism with a Jasco 720 spectropolarimeter with a red sensitive photomultiplier. Cell compartments were kept at 25°C with circulating water from thermostatted baths. Unless otherwise stated, by visible (vis) and circular dichroism (CD) spectra we mean a representation of $\varepsilon_m$ or $\Delta\varepsilon_m$ values vs $\lambda$ [$\varepsilon_m$ = absorption/($b \times C_{VO}$) and $\Delta\varepsilon_m$ = differential absorption/($b \times C_{VO}$); $b$ = optical path and $C_{VO}$ = total oxovanadium(IV) concentration]. The X-band ESR spectra were normally recorded at 77 K (on glasses made on freezing solutions in liquid nitrogen) with a Bruker ESR-ER 200tt connected to a B-MN C5 ESR spectrometer and to a Bruker ESR data system (linked to an IBM AT computer). Spectra were normally recorded varying the pH with approximately fixed total vanadium and ligand concentration, at several ligand-to-metal (L/M) ratios.

*TLC experiments*

These were performed on Merck TLC plates (Art. 5626, 10 × 20 cm). The ligands and solutions used for spectroscopic measurements were monitored to check their purity and reactions (e.g. hydrolysis) that might possibly occur during the experiments. Normally, 2 $\mu$l samples were applied to the plates 20 mm from the bottom. Elution was carried out in Camag twin chambers with walls covered with filter paper impregnated with the eluent. This was butanol–ethanol–propionic acid–water (10:10:2:5). When it reached ~120 mm from the bottom the plates were removed and dried. The chromatogram was developed with a ninhydrin–collidine (2,4,6-trimethylpyridine)–copper solution prepared according to Moffat and Lytle.[7] In some cases, after development with this solution, the plate was placed in an enclosed chamber for development with iodine vapours. Typically samples were taken for TLC after dissolution of the ligand, and addition of $VO^{2+}$ for several pH values.

## RESULTS

*3-Methyl-L-histidine + $VO^{2+}$ system*

Solutions of this amino acid gave only one reddish-brown spot in TLC experiments, and no decomposition of the ligand was detected throughout the measurements.

The ESR spectra with frozen "solutions" containing 3-methyl-L-histidine (3Mehis) and $VO^{2+}$ at 77 K for high L/M ratios are like those obtained in the L-histidine + $VO^{2+}$ system in similar experimental conditions throughout the whole pH range. The field region that corresponds to $A_\parallel$ and $M_I$ = 5/2 and 7/2 (3800/4300 Gauss) gives more information about the type and number of species present. Figure 1 shows some of the results in this field range. The only noticeable difference between these spectra and those for L-his[4,5] is that components IV are sharper and more symmetrical. Species IVA mentioned for the L-his + $VO^{2+}$ system[5] is either less important in the 3-Mehis + $VO^{2+}$ system, or cannot be distinguished from V and VI (Fig. 1).

Table 1 summarizes the relevant $g$ and $A$ ($\perp$ and $\parallel$) parameters calculated using the appropriate equations[8] based on Chasteen's method.[9] For most solutions at least two species are present and we have analysed these spectra as a superposition of two (or more) axial spectra. In some cases coincident perpendicular lines had to be assumed for the two (or more) species because these lines were not resolved in the spectra. In many cases even the parallel lines are close to each other, and the accuracy of the estimates of the spin Hamiltonian parameters is therefore affected. Despite this, the ESR parameters obtained for the 3Mehis + $VO^{2+}$ system (Table 1) are almost identical to those of the corresponding species in the L-his + $VO^{2+}$ system.[4,5]

The visible and CD spectra obtained for solutions containing **2** and $VO^{2+}$ are very similar to those for the L-his + $VO^{2+}$ system,[4,5] both in values of $\lambda_{max}$ and the corresponding $\varepsilon_m$ or $\Delta\varepsilon_m$. Consequently, we include no experimental spectra.

*1-Methyl-L-histidine + $VO^{2+}$ system*

Solutions of this amino acid corresponded to bluish-brown spots in TLC experiments; a small yellowish-white spot is detected above the amino acid spot for solutions also containing oxovandium(IV). No decomposition of the ligand was detected during the measurements.

Figure 2A shows some of the ESR spectra obtained for "solutions" containing 1-methyl-L-histidine (1Mehis) and $VO^{2+}$ at 77 K. For pH $\lesssim$ 3.6, the results are similar to those obtained for L-his and 3Mehis + $VO^{2+}$ in similar conditions. However, for pH $\gtrsim$ 3.7, the ESR spectra differ markedly. IV and VI are not detected and in the pH range 6–9 a different species, designated by VIII′, is dominant. At pH ~ 4.9 (Fig. 2), species designated by II′, III′ (and V′) are dominant and the field positions correspond to II, III and V in the L-his[4,5] and 3Mehis + $VO^{2+}$ systems. In the experimental conditions of Fig. 2, for pH $\gtrsim$ 8 the solutions become brown and for pH $\gtrsim$ 9.5 oligomeric species must form since the ESR signal almost disappears at pH ~ 11. Table 1 summarizes the relevant $g$ and

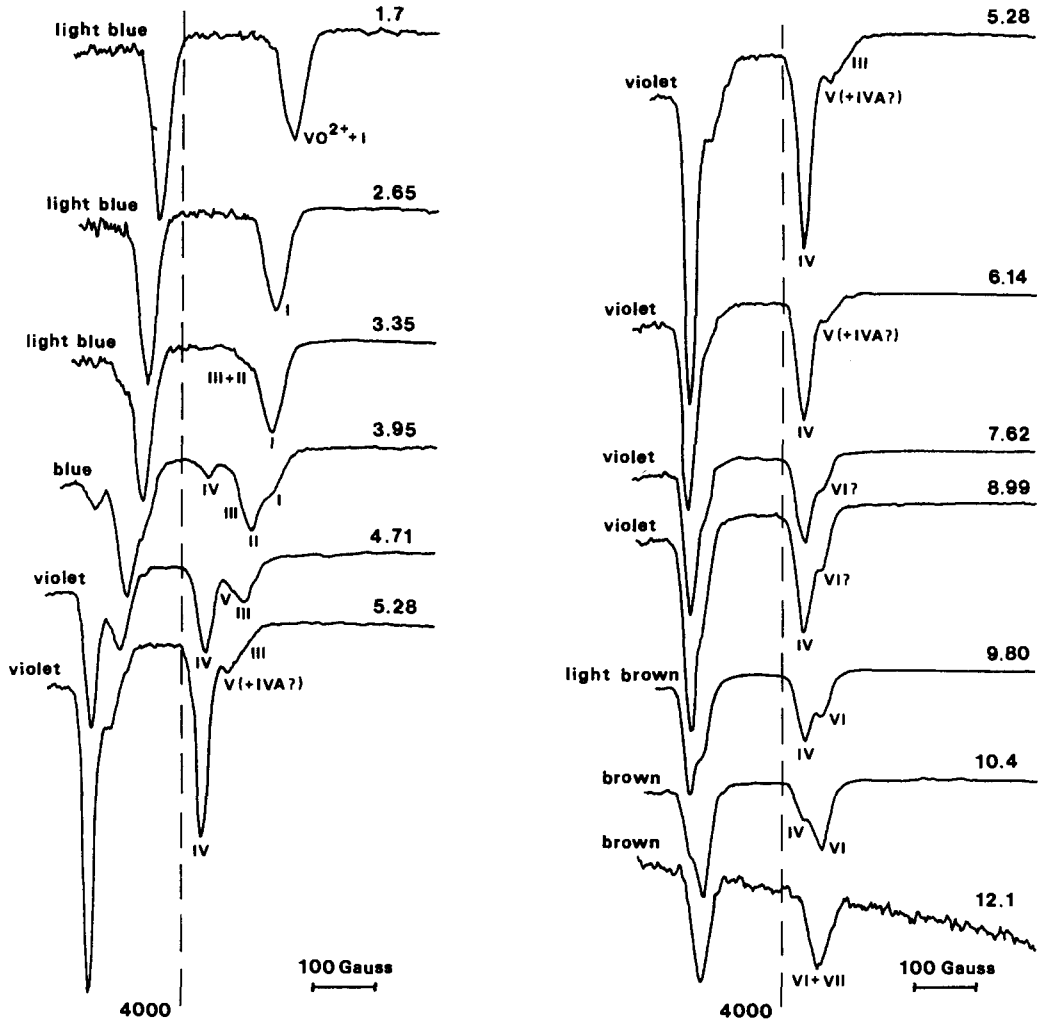


Fig. 1. High field range (3800–4400 Gauss) of the first derivative ESR spectra at 77 K of frozen "solutions" containing 3-methyl-L-histidine and $VO^{2+}$ with L/M = 9.63 and $C_{VO} \approx 0.011$–$0.012$ M. pH values and colours of the corresponding solutions are indicated.

$A$ ($\perp$ and $\|$) parameters calculated using the correct equations[8] based on Chasteen's[9] method.

The visible and CD spectra for solutions containing **3** and $VO^{2+}$ are quite different from those in the 3Mehis and L-his+$VO^{2+}$ systems in similar conditions.[4,5] Notably, the $\lambda_{max}$ (of the visible and CD spectra) differ and the $\Delta\varepsilon_m$ values are much lower (e.g. Figs 3 and 4).

### N$\alpha$-*Acetyl*-L-*histidine*

Solutions of this amino acid gave a single spot in TLC experiments ($R_f \sim 0.22$) after development with iodine vapour. No decomposition of the ligand was detected throughout the measurements.

Solutions containing *N*$\alpha$-acetyl-L-histidine (Achis) and $VO^{2+}$ (e.g. Figs 2B, 5 and 6) have a light blue colour till pH $\approx$ 4.5. This distinguishes them from those containing 3Mehis+$VO^{2+}$ in similar conditions, which at pH $\approx$ 3.8 are dark blue and for pH > 4.0–4.3 become violet. For pH $\gtrsim$ 4.8–5 the solutions become green (for the experimental conditions of Figs 2B, 5 and 6) and if the pH is not rapidly increased to 7–8, vanadyl hydroxide precipitates. For pH > 8, the solutions are greenish-brown but oxovanadium(IV) is extensively hydrolysed. The pH can then be decreased, the solutions become green, but the equilibria are sluggish and the visible and CD spectra recorded are irreproducible.

Figure 2B includes some of the ESR spectra. For pH $\gtrsim$ 6, the signal decreases and for pH $\gtrsim$ 9 no signal is detected [except for very high pH when $VO(OH)_3^-$ forms]. Table 1 includes ESR parameters calculated[8,9] for the species detected.

Figure 5 includes visible spectra for solutions

Table 1. Vanadium hyperfine coupling constants $A_{\parallel} \times 10^4/cm^{-1}$ and $g_{\parallel}$ values estimated[8,9] from the first derivative ESR spectra at 77 K of frozen "solutions" containing oxovanadium(IV) and L-histidine or related ligands using high L/M ratios (see text)

| L-Histidine | | 3-Methyl-L-histidine | | 1-Methyl-L-histidine | | Nα-Acetyl-L-histidine | | L-Histidine methyl ester | | L-Histidinol | | Histamine | |
|---|---|---|---|---|---|---|---|---|---|---|---|---|---|
| $A_{\parallel}$ | $g_{\parallel}$ | $A_{\parallel}$ | $g_{\parallel}$ | $A_{\parallel}$ | $g_{\parallel}$ | $A_{\parallel}$ | $g_{\parallel}$ | $A_{\parallel}$ | $g_{\parallel}$ | $A_{\parallel}$ | $g_{\parallel}$ | $A_{\parallel}$ | $g_{\parallel}$ |
| 179 | 1.938 | 182 | 1.933 | 181 | 1.936 | 183 | 1.930 | 183 | 1.932 | 182 | 1.929 | 183 | 1.930 |
| pH 1.9 | | pH 1.7 | | pH 1.9 | | pH 1.4 | | pH 3.3 | | pH 1.7–3.8 | | pH 1.7–3.9 | |
| 177 | 1.937 | 177 | 1.937 | 180 | 1.940 | 182 | 1.931 | | | | | | |
| pH 2.84 | | pH 2.65 | | pH 2.46 | | pH 2.0 | | | | | | | |
| 176 | 1.936 | 177 | 1.937 | 178 | 1.938 | 178 | 1.935 | | | 177–9 | ~1.936 | | |
| pH 3.36 | | pH 3.35 | | pH 3.58 | | pH 2.93 | | | | (I*) | | | |
| ~172 | ~1.945 | ~172 | ~1.947 | | | 175 | 1.936 | | | | | | |
| (II) | | (II) | | | | pH 4.34 | | | | | | | |
| ~170 | ~1.947 | ~171 | ~1.945 | ~170 | ~1.948 | 168–173 | — | | | | | | |
| (III) | | (III) | | pH 4.89 | | (IX″) | | | | | | | |
| 160–162 | ~1.953 | ~161 | ~1.957 | 163–4 | ~1.948 | | | ~162 | ~1.959 | ~163 | ~1.952 | ~162 | 1.945 |
| (IV) | | (IV) | | (VIII′) | | | | ($IV^{\oplus}$) | | (VII*) | | ($XII^{\#}$) | |
| ~166 | ~1.943 | ~166 | ~1.945 | ~150 | ~1.97 | 165 | 1.952 | ~165 | ~1.949 | 158–160 | ~1.953 | | |
| (V) | | (V) | | (Imp) | | pH 7–8 | | ($V^{\oplus} \simeq VI^{\oplus}$) | | (IX*) | | | |
| ~165 | ~1.946 | ~165 | ~1.953 | | | | | ~163 | ~1.949 | | | | |
| (VI) | | (VI) | | | | | | ($VII^{\oplus}$) | | | | | |

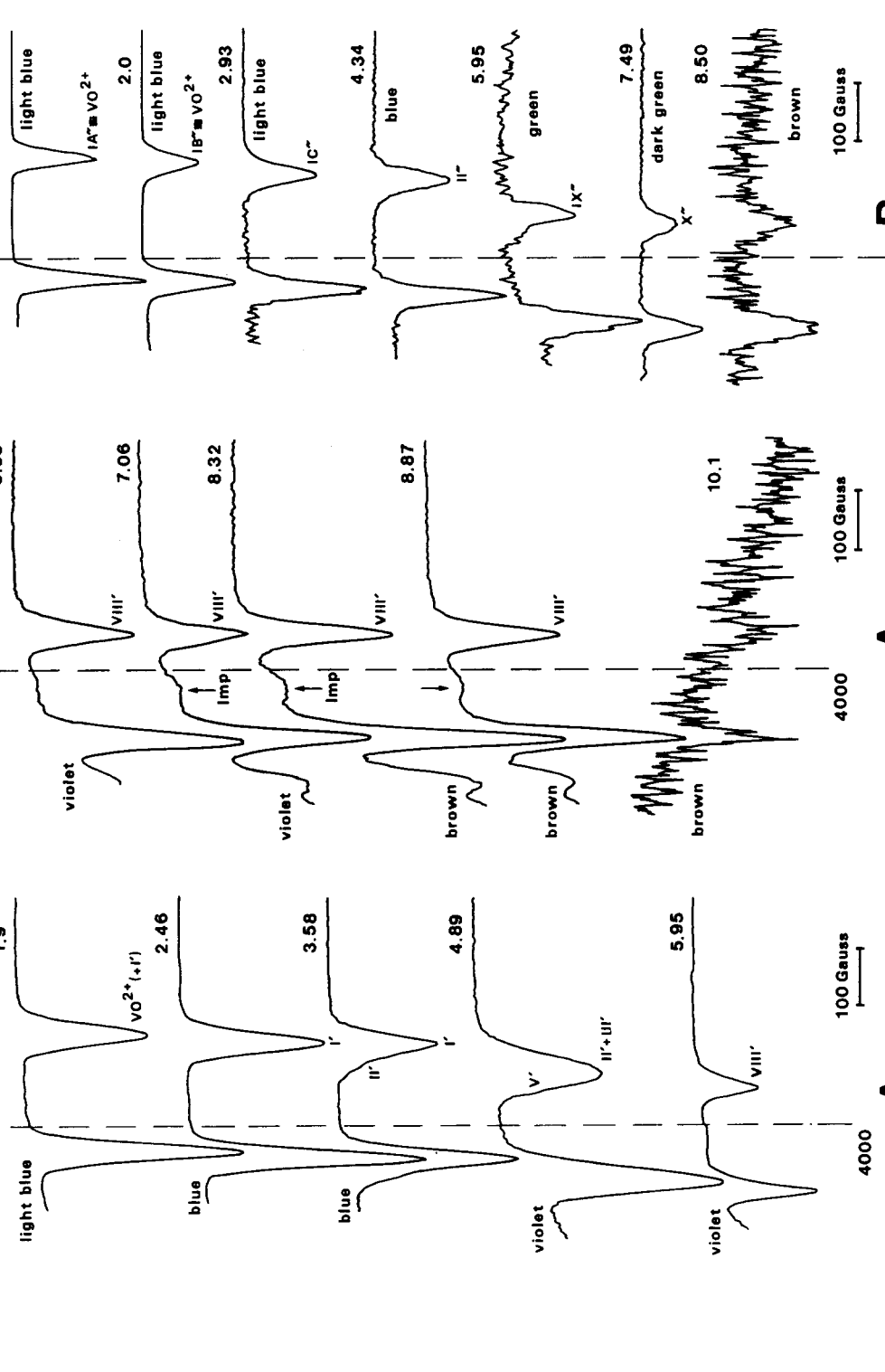


Fig. 2. High field range (3800–4400 Gauss) of the first derivative ESR spectra at 77 K of frozen "solutions". (A) 1-Methyl-L-histidine and $VO^{2+}$ with L/M = 10.1 and $C_{VO} \approx 0.011$–0.012 M. pH values and colours of the corresponding solutions are indicated. The visible and CD spectra of some of these solutions are included in Figs 3 and 4. For pH $\gtrsim$ 6, a signal designated by 'Imp' is detected. This possibly corresponds to an impurity of the ligand as, for this system, it is not possible to envisage any structure that could have such low $A_{\parallel}$ values. However, the possibility that these lines are due to the presence of a dimeric species in solution presenting a multiple-line ESR (e.g. 15-line) spectrum cannot be ruled out. (B) *N*α-Acetyl-L-histidine and $VO^{2+}$ with L/M = 15.0 and $C_{VO} \approx 0.012$–0.010 M. The visible and CD spectra of some of these solutions are included in Figs 5 and 6, respectively. For pH > 5, all spectra were recorded decreasing the pH from ~ 9.8, by addition of a relatively concentrated acid solution, avoiding significant change of volume.

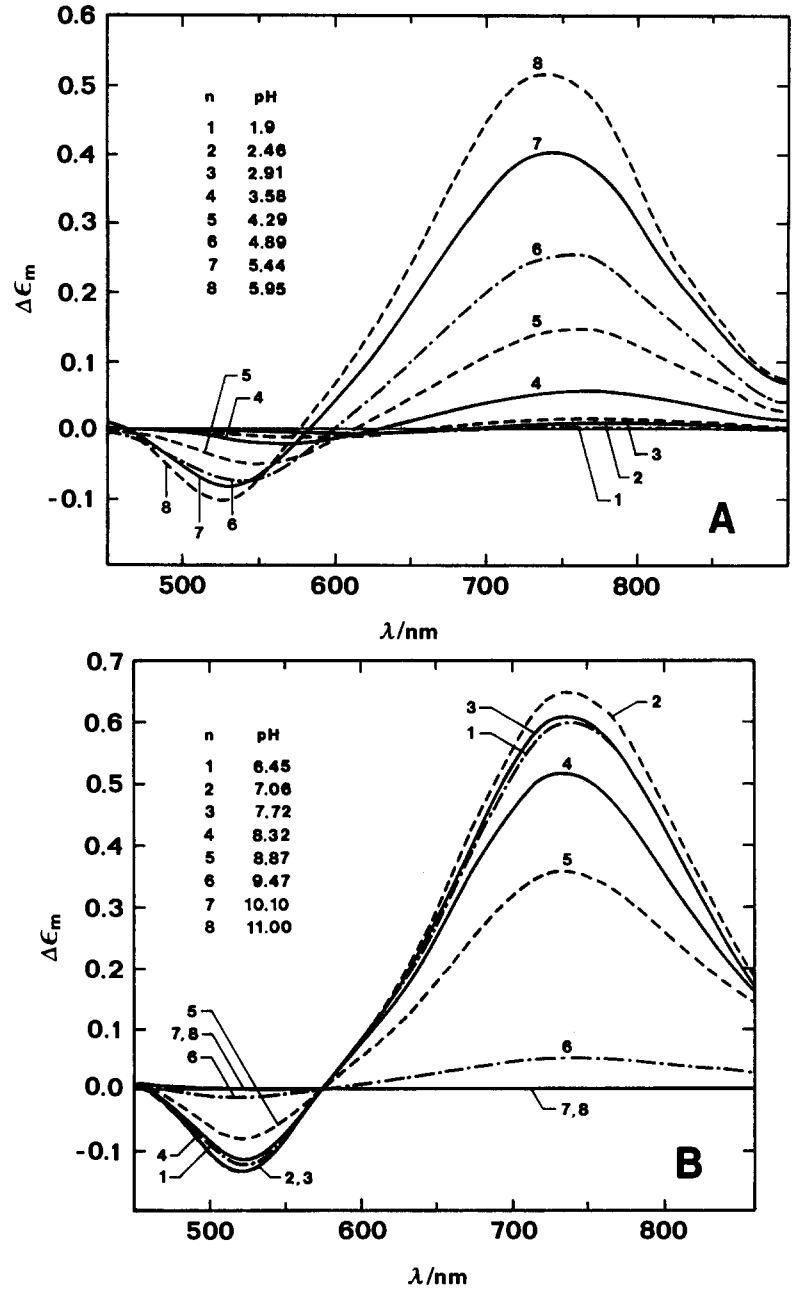


Fig. 3. CD spectra of solutions containing 1-methyl-L-histidine and $VO^{2+}$ with L/M = 10.1 and $C_{VO} \approx 0.012$–$0.011$ M. The pH corresponding to each spectrum is indicated. The ESR and visible spectra corresponding to some of these solutions are given in Figs 2A and 4, respectively. The representation of $\Delta\varepsilon_m$ as pH is varied is given in Fig. 14B.

containing **6** and $VO^{2+}$. These are quite different from those for the L-his, 3-Mehis and 1-Mehis + $VO^{2+}$ systems, but are relatively similar to those for the glycylglycine and glycylglycylglycine + $VO^{2+}$ systems[10] in similar conditions. Figure 6 includes CD spectra for solutions containing **6** and $VO^{2+}$. These spectra also differ completely from those obtained for the L-his, 3Mehis and 1Mehis + $VO^{2+}$.

*L-Histidine methyl ester*

TLC chromatograms of solutions containing L-histidine methyl ester (HisME) showed three spots: (1) due to L-his (violet; weak; $R_f \sim 0.04$), (2) due to **4** (brownish-violet; strong; $R_f \sim 0.18$), (3) due to an unknown compound (brownish-yellow; weak; $R_f \sim 0.27$). The addition of oxovanadium(IV) apparently does not change their relative intensities.

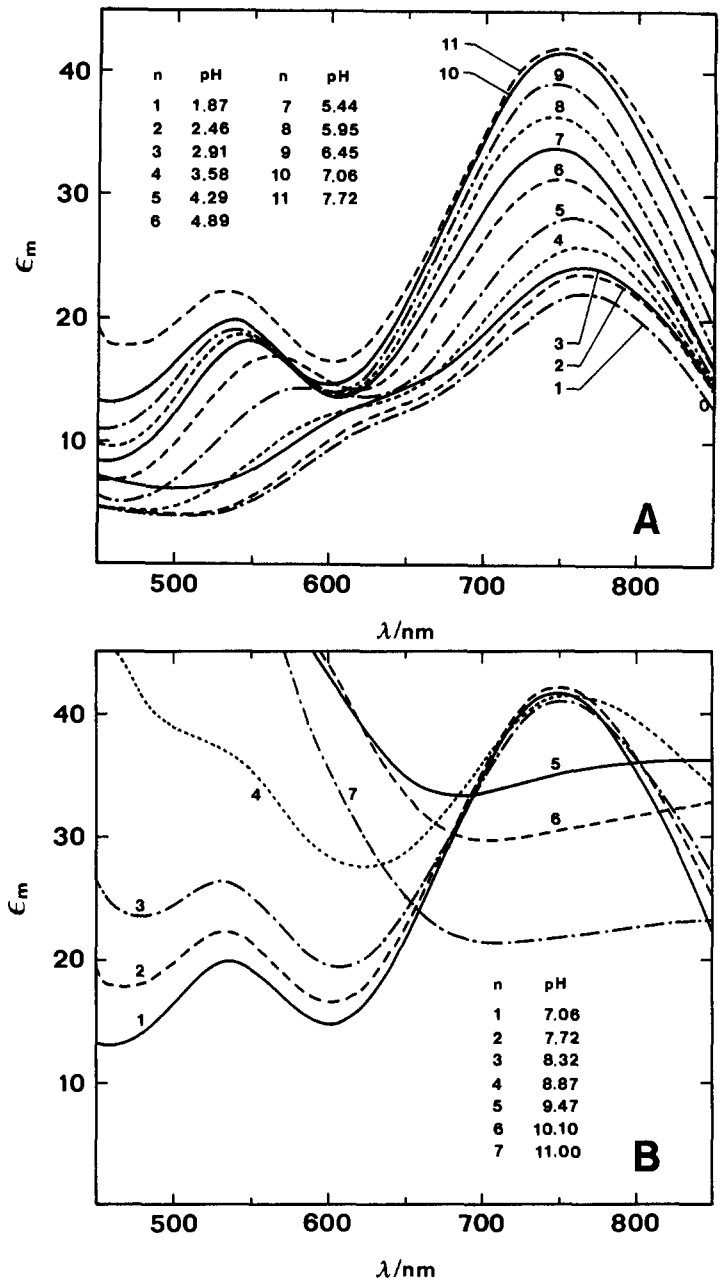


Fig. 4. Visible absorption spectra of solutions containing 1-methyl-L-histidine and $VO^{2+}$ with L/M = 10.1 and $C_{VO} \approx 0.012$–$0.011$ M. The pH corresponding to each spectrum is indicated. The ESR and CD spectra corresponding to some of these solutions are given in Figs 2A and 3, respectively.

At pH ~ 10, the intensity of the L-his spot increases slowly with time and after ~2 h a new brownish-yellow spot is detected at $R_f \sim 0.09$.

Solutions containing **4** and $VO^{2+}$ with high L/M ratios, in experimental conditions similar to those of Figs 7–10, are light blue up to pH ≈ 4. For pH > 4.1–4.3 (depending on experimental conditions), vanadyl hydroxide may precipitate if the pH is not rapidly increased to ~7.5. For pH > 8, the solutions are grey–violet and for pH > 8.5–9 they become brown, indicating extensive oxovanadium(IV) hydrolysis.

Figure 7A includes some of the ESR spectra. For pH < 3.5, the ESR parameters (Table 1) are consistent with the existence of $[VO(OH_2)_5]^{2+}$. For pH > 5–6, the present spectra show some similarities to those found for the L-his[4,5] and 3Mehis + $VO^{2+}$ systems, but the species designated

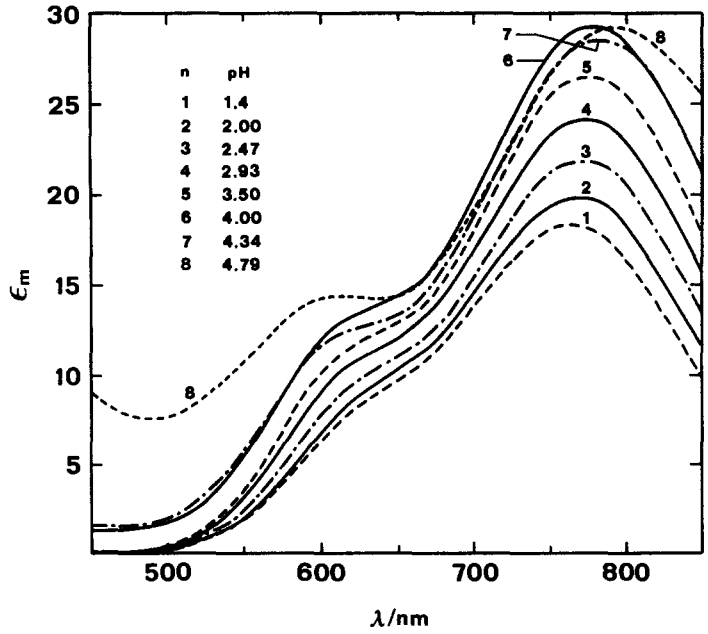


Fig. 5. Visible absorption spectra of solutions containing *N*α-acetyl-L-histidine and $VO^{2+}$ with L/M = 15.0 and $C_{VO} \approx 0.012$–0.011 M. The pH corresponding to each spectrum is indicated. The ESR and CD spectra corresponding to some of these solutions are given in Figs 2B and 6, respectively.

by $IV^{\oplus}$ is much less important than for L-his and 3Mehis + $VO^{2+}$. The estimated ESR parameters are given in Table 1.

Figures 8 and 9 include some of the visible and CD spectra for solutions containing **4** and $VO^{2+}$. The pH was progressively increased from ~1.7 to 4.1, and spectra were recorded every 0.5 pH units. At pH ~ 4.1, after ~15 min vanadyl hydroxide began precipitating. Base was added till pH ~ 7.4, the very small amount of precipitate that had formed dissolved and the solution became greyish-violet. Spectra were recorded every 0.4–0.5 pH units till pH ~ 10, and then acid was added till pH ~ 6. Spectra were then recorded every 0.5 pH units till pH ~ 4.6.

For pH > 3, the CD (and visible) spectra differ from those for the L-his[4,5] and 3Mehis + $VO^{2+}$ systems in similar conditions. In particular, the maximum values of $\Delta\varepsilon_m$ (band I) in the pH range 5–7 are ~85% of the counterparts for solutions containing L-his or 3Mehis + $VO^{2+}$. In the pH range 7–8, a band with $\Delta\varepsilon_m > 0$ is seen in the CD spectra of Fig. 9B. No such band is detected for the L-his[4,5] and 3Mehis + $VO^{2+}$ solutions.

### L-*histidinol*

Solutions of this amino acid in TLC experiments showed a major violet spot at $R_f \sim 0.06$ and a yellowish-white spot at $R_f \sim 0.13$. No decomposition of the ligand was detected throughout the measurements.

Solutions containing **5** and $VO^{2+}$ with high L/M ratios in conditions like those of Figs 7, 10 and 11 are light blue up to pH ≈ 4, when they become dark blue. For pH > 4.0–4.2 (depending on conditions), vanadyl hydroxide may precipitate if the pH is not rapidly increased to ~8. For pH > 8, the solutions are light brown and the colour darkens for pH > 10, indicating extensive oxovanadium(IV) hydrolysis, also evident from the visible spectra (Fig. 10). On acidifying the solution corresponding to spectrum no. 16 in Fig. 11C, it becomes dark green at pH ≈ 7.8. At pH ≈ 7 vanadyl hydroxide precipitates.

Figure 7B includes some of the ESR spectra. For pH < 3.8, the estimated $g$ and $A$ (⊥ and ‖) parameters for the main species detected (Table 1) are consistent with the formation of $[VO(OH_2)_5]^{2+}$. For pH > 8, the spectra differ from those found for the L-his[4,5], 3Mehis and HisME + $VO^{2+}$ systems. The species designated by IV* is much less important in the present system than IV in the L-his and 3Mehis + $VO^{2+}$ systems (e.g. Fig. 1). The estimated[8,9] ESR parameters are given in Table 1.

Although the CD spectra for pH ≲ 2.2 (Fig. 11A) resemble those for the HisME + $VO^{2+}$ system in similar conditions, most of the CD spectra are quite different from those for the other systems. In Fig. 11B, the pattern of the spectra clearly changes

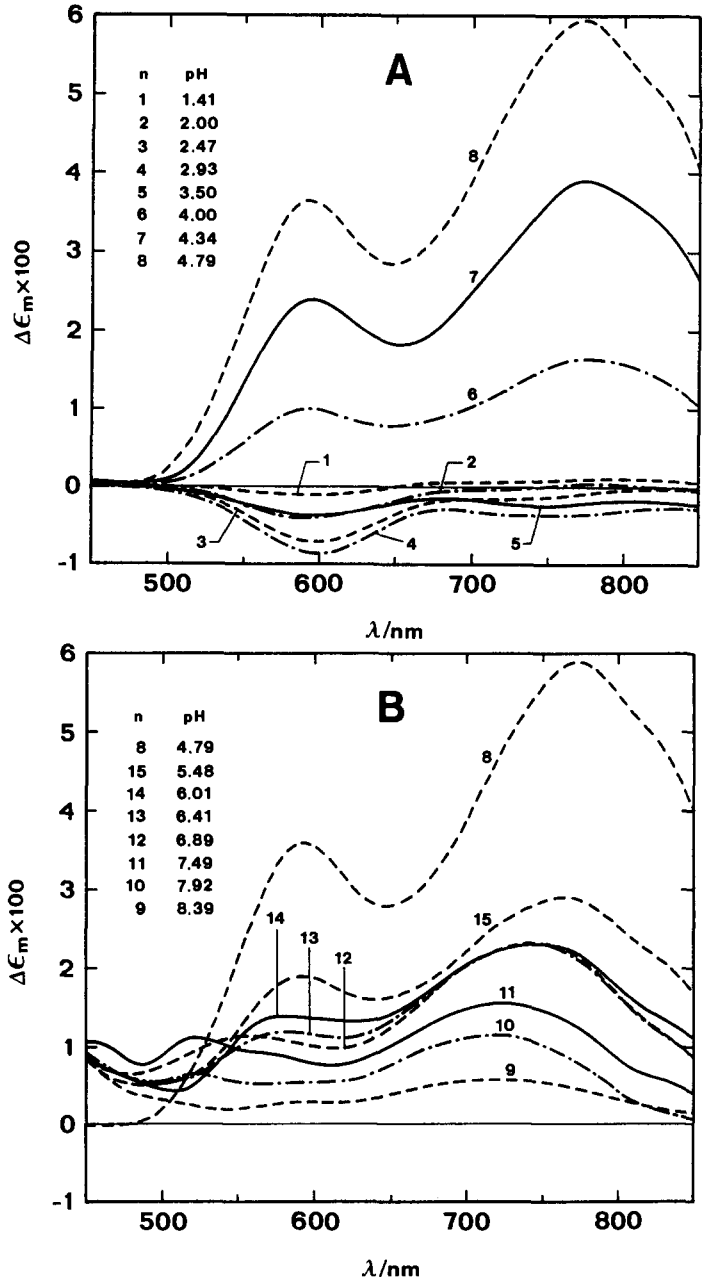


Fig. 6. CD spectra of solutions containing *N*α-acetyl-L-histidine and $VO^{2+}$ with L/M = 15.0 and $C_{VO} \approx 0.012$–$0.011$ M. The pH corresponding to each spectrum is indicated. The ESR and CD spectra corresponding to some of these solutions are given in Figs 2B and 5, respectively. Spectra 9–15 were recorded following this order, i.e. by successive addition of acid. As mentioned in the text the equilibria are sluggish, the spectra are not reproducible from batch to batch, but their general pattern is the same for each pH. The representation of $\Delta\varepsilon_m$ as pH is varied is given in Fig. 14A.

drastically as pH is increased from 8.3 to 9.9, an isodichroic point being detected at ~628 nm. Therefore, although no clear modifications are seen in the corresponding ESR (Fig. 7B) and visible (Fig. 10B) spectra, these CD spectra suggest the existence of an equilibrium between (at least) two optically active complexes. This involves VII* (and IV*; VI*) and IX*. Besides the colours (and spectra) of the solutions, the relatively low $\Delta\varepsilon_m$ values indicate that vanadium is quite extensively hydrolysed in these conditions. For pH > 10, there is a general decrease in the $\Delta\varepsilon_m$ values as pH is increased, indicating further hydrolysis and gradual substitution of **5** by $OH^-$.

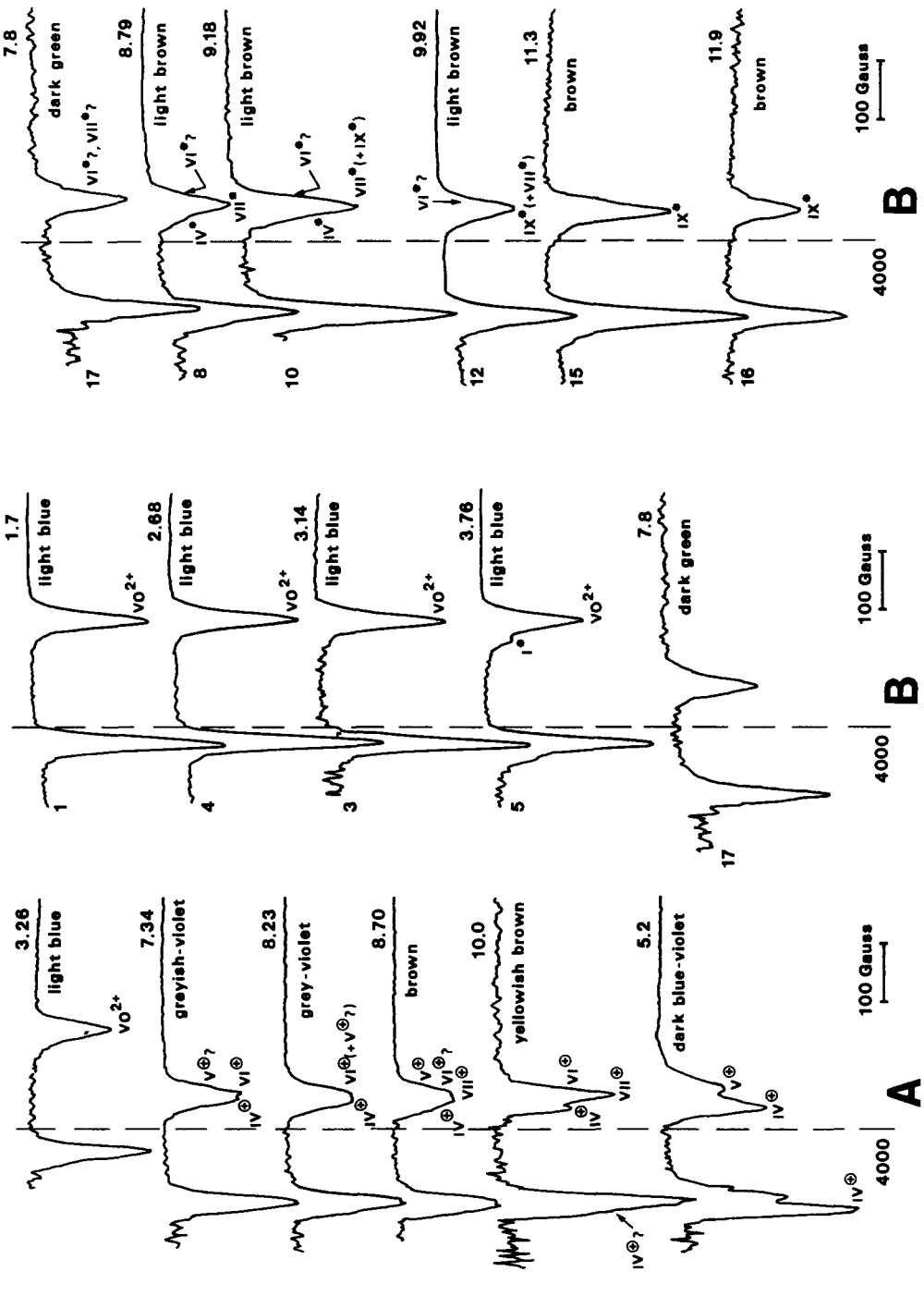


Fig. 7. High field range (3800–4400 Gauss) of the first derivative ESR spectra at 77 K of frozen "solutions". (A) L-Histidine methyl ester and $VO^{2+}$ with L/M = 20.0 and $C_{VO} \approx 0.015$–0.008 M. The solution corresponding to the spectrum at pH 5.2 was prepared by acidifying solutions with higher pH (see text). The species detected at field positions similar to those of solutions containing L-his or 3Mehis + $VO^{2+}$ (e.g. Fig. 1, IV) are designated by the same symbol but with a superscript⊕ (e.g. $IV^{\oplus}$). The visible and CD spectra corresponding to some of these solutions are given in Figs 8 and 9, respectively. (B) L-Histidinol and $VO^{2+}$ with L/M = 15.2 and $C_{VO} \approx 0.018$–0.014 M. Species IV* and VII* are also labelled because their field positions are identical to those of IV and VII in the ESR spectra of L-his or 3Mehis + $VO^{2+}$ (cf. Fig. 1). The visible and CD spectra corresponding to some L-histidinol solutions are included in Figs 10 and 11. The solution corresponding to the spectrum at pH 7.8 was prepared by acidifying the solution with pH 11.9.

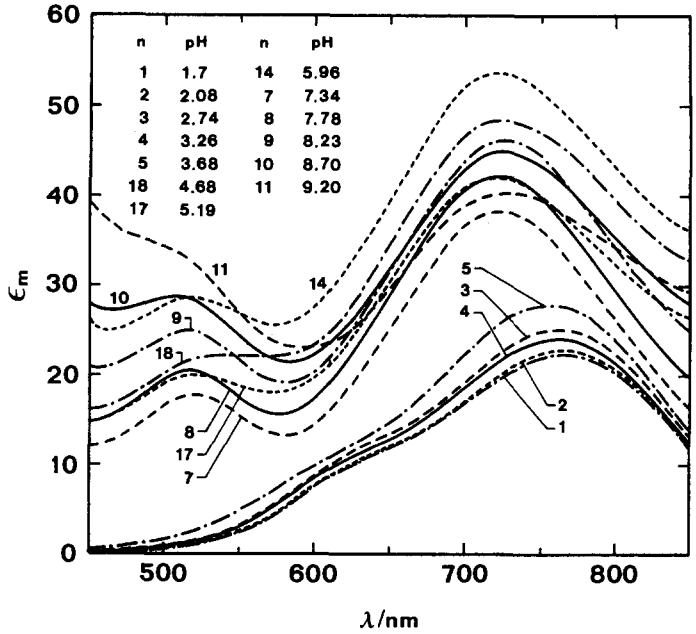


Fig. 8. Visible absorption spectra of solutions containing L-histidine methyl ester and $VO^{2+}$ with L/M = 20.0 and $C_{VO} \approx 0.015$–$0.008$ M (see text for details). The pH corresponding to each spectrum is indicated. The spectra are numbered in their order of recording. The ESR and CD spectra corresponding to some of these solutions are given in Figs 7A and 9, respectively.

*Histamine*

Solutions of **7** gave a single spot (brown or brownish-yellow, depending on the amount applied) in TLC experiments. No decomposition of the ligand was detected by TLC throughout the measurements.

Solutions containing **7** and $VO^{2+}$ with high L/M ratios in conditions similar to those of Figs 12 and 13 have a light blue colour up to pH $\approx$ 4. For pH > 4, vanadyl hydroxide precipitates if the pH is not rapidly increased above ~8. For pH > 8, the solutions are brown, indicating extensive oxovanadium(IV) hydrolysis, also evident from the visible spectra (Fig. 13). Acidifying the solution corresponding to spectrum no. 8 in Fig. 13, for pH < 8, vanadyl hydroxide precipitates.

Figure 12 includes some ESR spectra. For pH < 3.8, the estimated $g$ and $A$ ($\perp$ and $\parallel$) parameters for the main species detected (Table 1) are consistent with the formation of $[VO(OH_2)_5]^{2+}$. For pH > 8, the spectra differ from those for the other systems in this study, and at pH 8.3 only one species is detected, designated by VII#. The ESR signal is much weaker than at lower pH, consistent with hydrolysis of oxovandium(IV), forming oligomeric species which are ESR silent.

Figure 13 includes some visible spectra of solutions containing **7** and $VO^{2+}$. Up to pH ~ 3.5, the $\varepsilon_m$ values are almost identical with those for $[VO(OH_2)_5]^{2+}$. At pH ~ 3.9, the general increase in the $\varepsilon_m$ values is consistent with the hydrolysis and formation of $[(VO)_2(OH)_2]^{2+}$ (and $[VO(OH)]^+$).[11] For pH > 8, band II cannot be located and $\lambda_{max}$ (band I) shifts to the red.

## DISCUSSION

We have recently investigated[4,5] the L-histidine + $VO^{2+}$ system in aqueous solution by combining the results of potentiometric and spectroscopic techniques, and proposed an equilibrium model including species $MLH_2$, MLH, $MLH_{-2}$, $ML_2H_4$, $ML_2H_3$, $ML_2H_2$, $ML_2H$, $ML_2$, $ML_2H_{-1}$ and $M_2L_2H_{-4}$. Isomeric structures for each stoichiometry were discussed, but it was important to clarify these for some species.

Several potentiometric and spectroscopic studies have been reported on the $Cu^{II}$ + L-his and related systems, particularly using CD techniques.[11–13] Most used L/M ratios of 2 and involved comparisons with binary and ternary systems. However, with $VO^{2+}$, studies involving solutions with L/M = 2 are possible only with very extensive hydrolysis of the metal ion: even when using high L/M ratios to prevent this, more than one stoichiometry is normally present at any pH value. Besides, due to the existence of the V=O bond, the number of possible isomeric structures is often

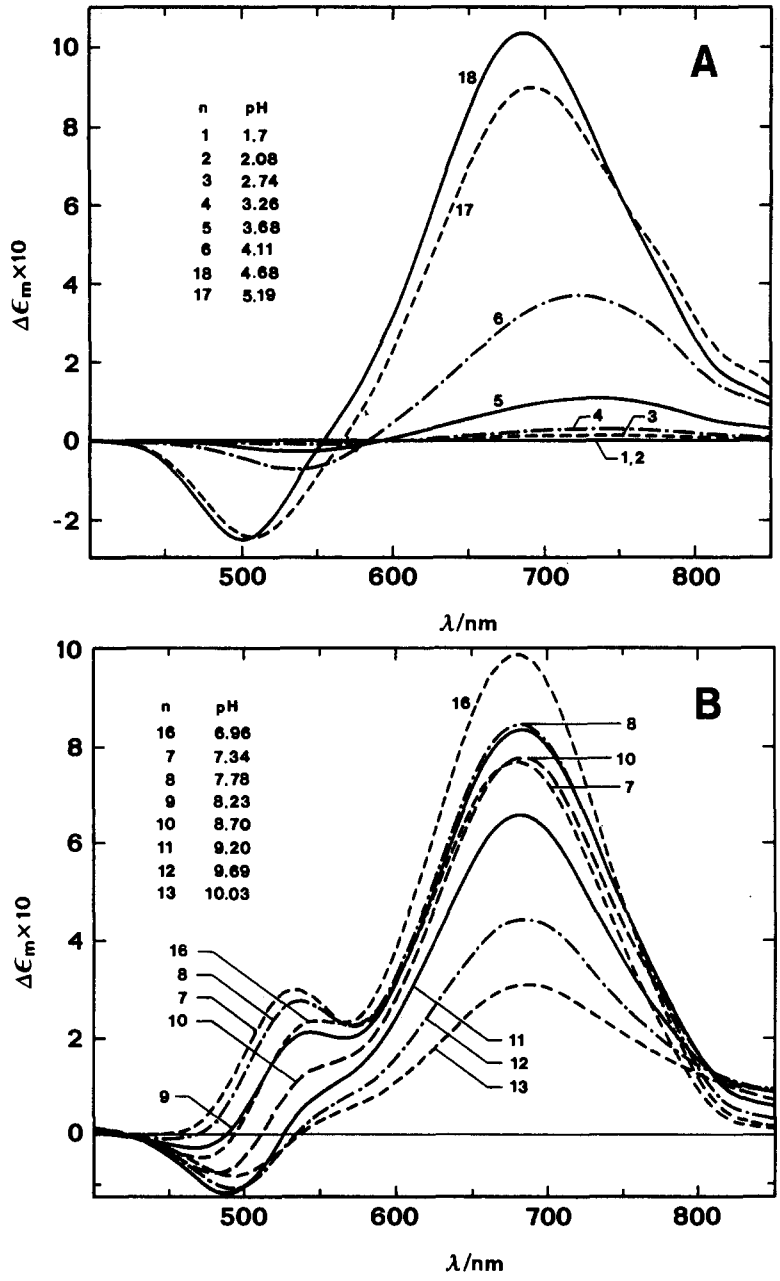


Fig. 9. CD spectra of solutions containing L-histidine methyl ester and $VO^{2+}$ with L/M = 20.0 and $C_{VO} \approx 0.015$–$0.008$ M (see text for details). The pH corresponding to each spectrum is indicated. The spectra are numbered in the order of recording; $\Delta\varepsilon_m$ values for spectra 1–6 are multiplied by a factor of 2. Some corresponding ESR and visible spectra are given in Figs 7A and 8, respectively. The representation of $\Delta\varepsilon_m$ as pH is varied is given in Fig. 14D.

greater than for $Cu^{II}$ complexes.[6,14] Consequently, what was done for the $Cu^{II}$ systems [11–13] is not possible for vanadium: that would include the use of additive functions of independent contributions from groups present in the molecules or any detailed discussion about the origins of particular CD bands. However, comparisons between the pH dependence of the visible CD, visible isotropic absorption and ESR spectra obtained for the L-histidine+$VO^{2+}$ system and those for the corresponding spectra for several L-histidine derivatives and related ligands included in this work allow some clarification of the coordination modes. Representations of $\Delta\varepsilon_m$ values as pH is varied, such as those shown in Fig. 14, are also useful to detect the formation and disappearance of complex species in solution.

We now discuss, on the basis of the present ESR,

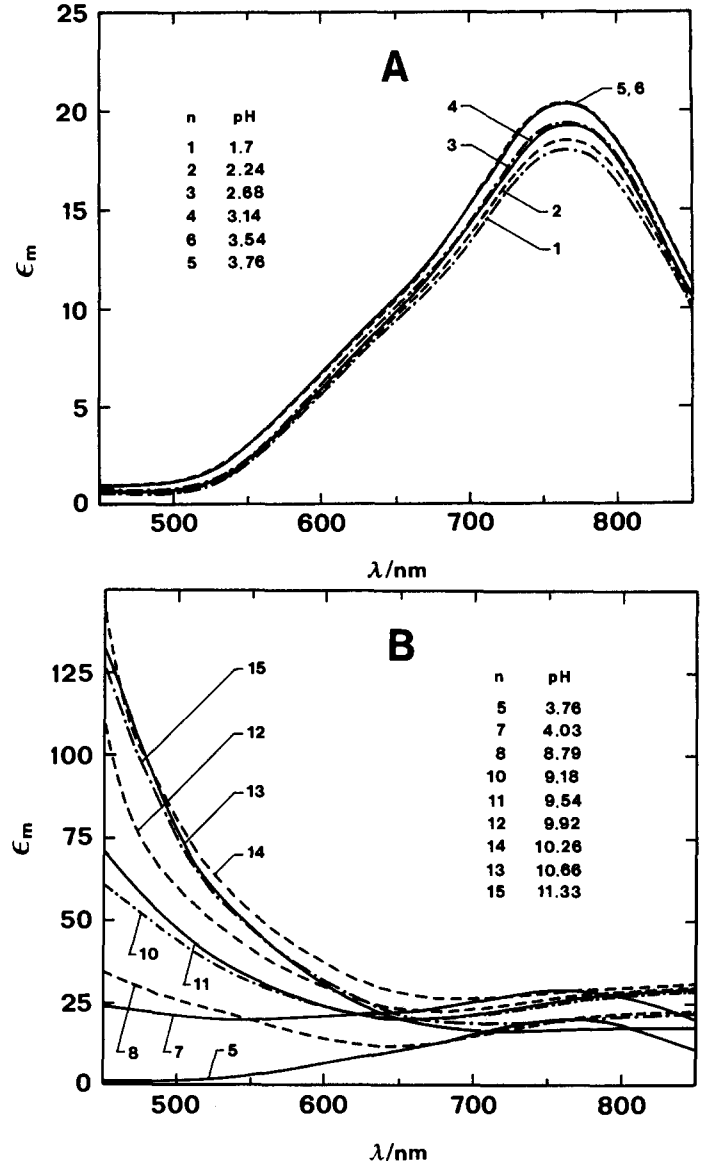


Fig. 10. Visible spectra of solutions containing L-histidinol and $VO^{2+}$ with L/M = 15.3 and $C_{VO} \approx 0.018$–$0.015$ M (see text for details). The pH corresponding to each spectrum is indicated. Some corresponding ESR and visible spectra are given in Figs 7B and 11, respectively.

visible and CD spectra and those for L-his + oxovanadium(IV),[4,5] structures for the complexes present in the several systems.

### 3-*Methyl*-L-*histidine*

The ESR, visible and CD spectra for solutions containing **2** and $VO^{2+}$ closely resemble those for the L-his $+VO^{2+}$ system,[4,5] and the $A_{\parallel}$ and $g_{\parallel}$ parameters for the corresponding species in the two systems are almost identical (e.g. Table 1). Therefore, apart from small differences that may exist in the ratios of isomeric structures for particular stoichiometries, all results indicate that the mode of coordination of both ligands throughout the pH range up to at least 11–12 is the same. In particular, it may be concluded that no deprotonation/coordination of the imidazole N(3)H (pyrrole NH) occurs (no comparative studies were done for pH > 12).

### Nα-*Acetyl*-L-*histidine*

The type of results obtained for this system (see above) and the fact that for pH $\gtrsim$ 3.5 the ESR, visible and CD spectra are quite different from those for the L-his and 3Mehis + $VO^{2+}$ confirms

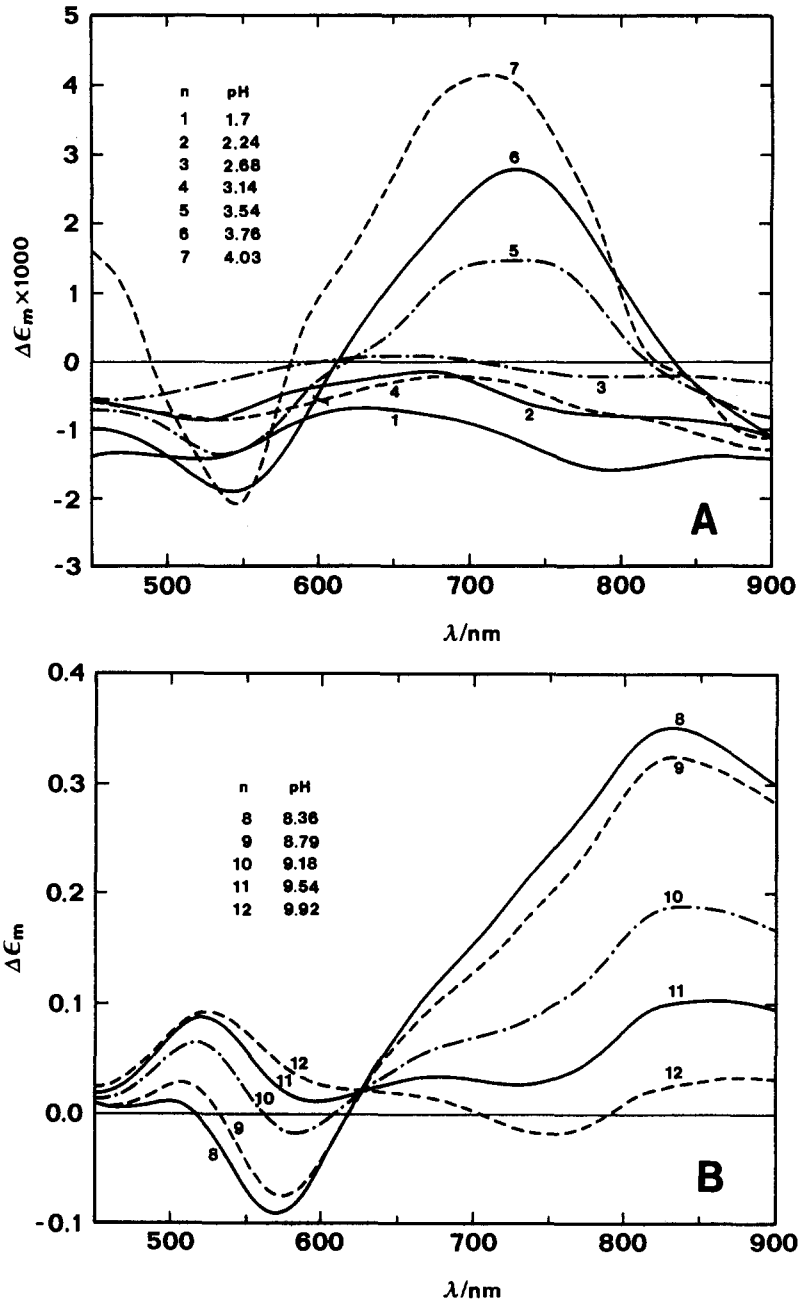


Fig. 11. CD spectra of solutions containing L-histidinol and $VO^{2+}$ with L/M = 15.3 and $C_{VO} \approx 0.018$–0.015 M (see text for details). The pH corresponding to each spectrum is indicated. The ESR and visible spectra corresponding to some of these solutions are given in Figs 7B and 10, respectively. The representation of $\Delta\varepsilon_m$ as pH is varied is shown in Fig. 14C and E.

that the amino nitrogen ($N_{am}$) in the latter coordinates.

At pH ~ 1.4, the estimated $g$ and $A$ ($\perp$ and $\parallel$) parameters for species IA″ (Fig. 2B and Table 1) are consistent with the formation of $[VO(OH_2)_5]^{2+}$. For pH < 3 (e.g. Figs 2B, 5 and 6A) the results are consistent with the simultaneous existence of the aqua ion and of carboxylate complexes **8** (and **9** in lower concentration; Table 2).

For pH > 3, the $\Delta\varepsilon_m$ values start to increase (e.g. Figs 6A and 14A). At pH 3.5 they are still <0, but at pH 4.0 (spectrum no. 6) two bands with $\Delta\varepsilon_m > 0$ are clearly seen, with $\lambda_{max}$ (band I) ~775 and $\lambda_{max}$ (band II) ~590 nm. A different species forms (II″ in the ESR): this dominates the pattern of the CD spectra in the pH range 4.0–4.8. Assuming that the imidazole nitrogen ($N_{im}$) has a contribution to the $A_{\parallel}$ values identical to the bipyridyl nitrogen atoms

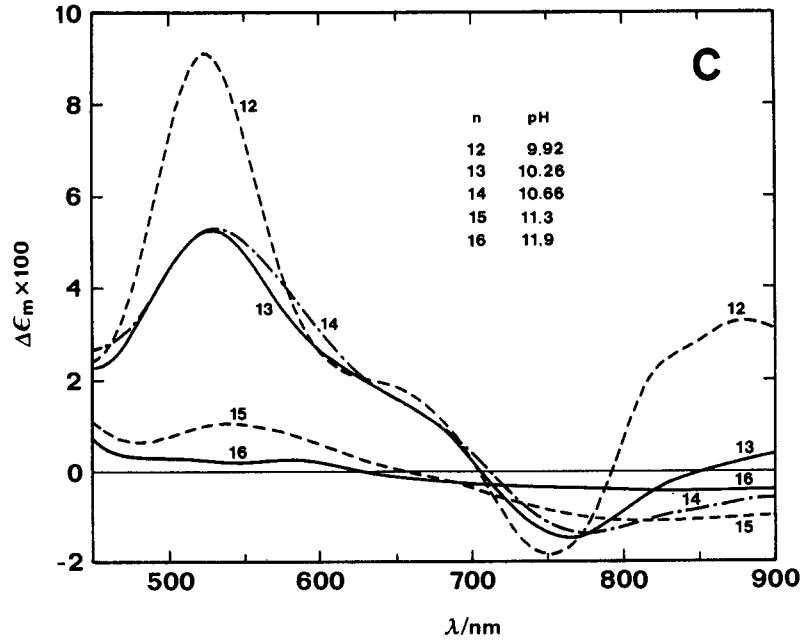


Fig. 11—*continued.*

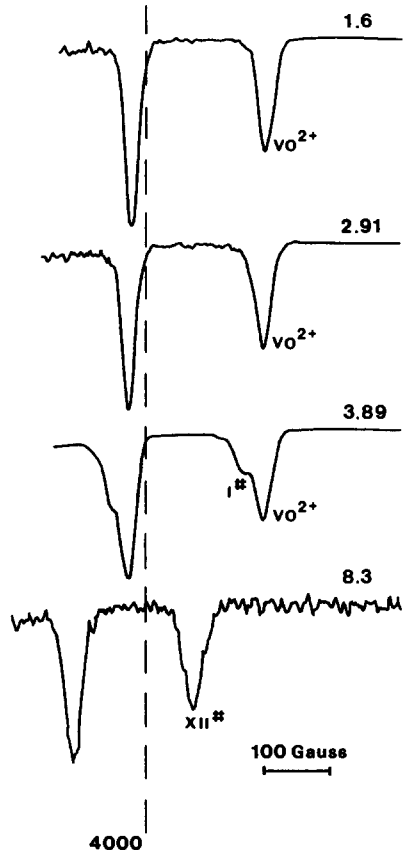


Fig. 12. High field range (3800–4400 Gauss) of the first derivative ESR spectra at 77 K of frozen "solutions" containing histamine and $VO^{2+}$ with L/M = 22.4 and $C_{VO} \approx 0.018$–$0.014$ M. Up to pH ~ 3.9, these were light blue; at pH ~8.3 the solution is brown. The corresponding visible spectra are shown in Fig. 13.

($162.8 \times 10^{-4}$ $cm^{-1}$),[9] the ESR parameters for II″ (Fig. 2B and Table 1) are consistent with the formation of a complex with two $H_2O$, one $COO^-$ and $N_{im}$ coordinated in equatorial positions. Structures **10** and **11** can then be envisaged for this species. In **10**, the equatorial bidentate coordination of $COO^-$ and $N_{im}$ involves a seven-membered chelate ring, normally not very favourable. This may explain why for pH > 4.8 oxovanadium(IV) is very extensively hydrolysed and eventually vanadyl hydroxide precipitates.

One must also emphasize that structure **9** (and possibly **12**) is also reasonable. In fact, the pattern of the CD spectrum for the corresponding species in the L-ala[6] and L-ser[15] + $VO^{2+}$ systems has some similarities with that in the pH range 3–4.8 shown in Fig. 6A. Besides, the visible spectra for pH < 4.8 (e.g. Fig. 5) do not indicate equatorial coordination of a nitrogen atom. Dessi *et al.*[16] also explain ESR spectra of solutions containing *N*-acetyl-glycine with L/M = 77 for pH < 6 assuming the formation of complexes such as **9** (Table 2).

At pH 5.95, species IX″ is detected in the ESR, but a significant fraction of oxovandium(IV) is in oligomers. The ESR signal is weak and the accuracy of its parameters is correspondingly low. The ESR-active species could have coordination geometries such as **13** and **14**. For pH > 7, the $A_{\parallel}$ values of the ESR-active species decrease further. The $\Delta\varepsilon_m$ values continue to decrease and $\lambda_{max}$ (bands I) shifts to the UV (Figs 6B and 14A). The absorbance for $\lambda < 550$ nm increases significantly and consequently the decreased accuracy of the CD spectra in this range precludes the determination of the true behaviour

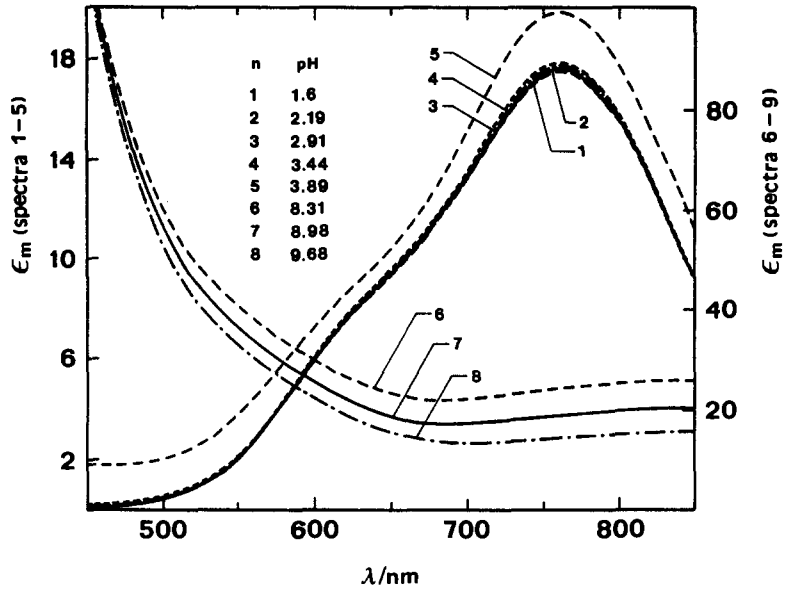


Fig. 13. Visible absorption spectra of solutions containing histamine and $VO^{2+}$ with L/M = 22.4 and $C_{VO} \approx 0.018$–$0.015$ M (see text for details). The pH corresponding to each spectrum is indicated. Some related ESR spectra are shown in Fig. 12. Spectra 1–5 and 6–8 have different $\varepsilon_m$ scales.

of band II. These results are consistent with the progressive equatorial coordination of $OH^-$ ligands till oxovanadium(IV) is completely hydrolysed.

### l-*Methyl*-L-*histidine*

The results for this system are similar to those for L-ala + oxovanadium(IV),[6] implying coordination as a simple α-amino acid. The spectra differ greatly from those for the L-his and 3Mehis + $VO^{2+}$ systems. This further indicates coordination of $N_{im}$ in those systems, where it is important in preventing oxovanadium(IV) hydrolysis as pH is increased.

At pH ~ 1.9, the estimated ESR parameters (Fig. 2A and Table 1) are consistent with the formation of $[VO(OH_2)_5]^{2+}$, the carboxylate complexes **8** probably existing in lower concentration. At pH 2.46 and 3.58 (Fig. 2A), the ESR spectra are consistent with the formation of the aqua ion and of carboxylate complexes **8** (and **9** in lower concentration). At pH 3.58, a second distinct species, designated by II′, is detected. In the corresponding visible and CD spectra (spectra no. 4 in Figs 3A and 4A) band II shifts to the UV and $|\Delta\varepsilon_m|$ values increase significantly (Fig. 14B). These observations are consistent with the formation of **15** (and **16**; Table 2).

At pH > 6, only one species is detected in the ESR spectra; this is designated by VIII′ in Fig. 2A. The corresponding ESR parameters, visible and CD spectra are similar to those obtained for $[VO(L\text{-}ala)_2]$,[6] except that the $|\Delta\varepsilon_m|$ values of band I are about twice those for the bis-alaninato complex. Therefore, VIII′ probably corresponds to structure **17**; at higher values of pH structures such as **18** could also be important. For pH > 10, oligomeric species form: the ESR and CD signals disappear (Figs 2A, 3B and 14B) and the visible spectra change, as found for the other systems where oxovanadium(IV) hydrolyses extensively.

### L-*Histidinol*

In the pH range 1.7–3.8, the estimated $g$ and $A$ ($\perp$ and $\parallel$) parameters for the main species detected (Fig. 7B and Table 1) are consistent with the formation of $[VO(OH_2)_5]^{2+}$. This agrees with the very low $\Delta\varepsilon_m$ values observed (Figs 11A and 14C, E) and with the visible spectra recorded (Fig. 10A). At pH 3.76, species I* is detected. The $|\Delta\varepsilon_m|$ values also increase significantly. Species I* could arise from an impurity, i.e. a small amount of histidine which at this pH would be in the form I (Fig. 1). As the $R_f$ of **5** and **1** are similar, a small percentage of this ligand could hardly be detected by TLC. However, I* could also correspond to **19** whose estimated[9] ESR parameters are approximately the same.

The CD spectra recorded in the pH range 3.5–4 suggest the formation of a very small amount of complexes involving the bidentate coordination of the ligand. At pH ~ 4, vanadium is very extensively hydrolysed and vanadyl hydroxide starts precipitating after several minutes. If base is added till pH ~ 8–9, the precipitate dissolves and the ESR and CD spectra become quite different (Figs 7B and

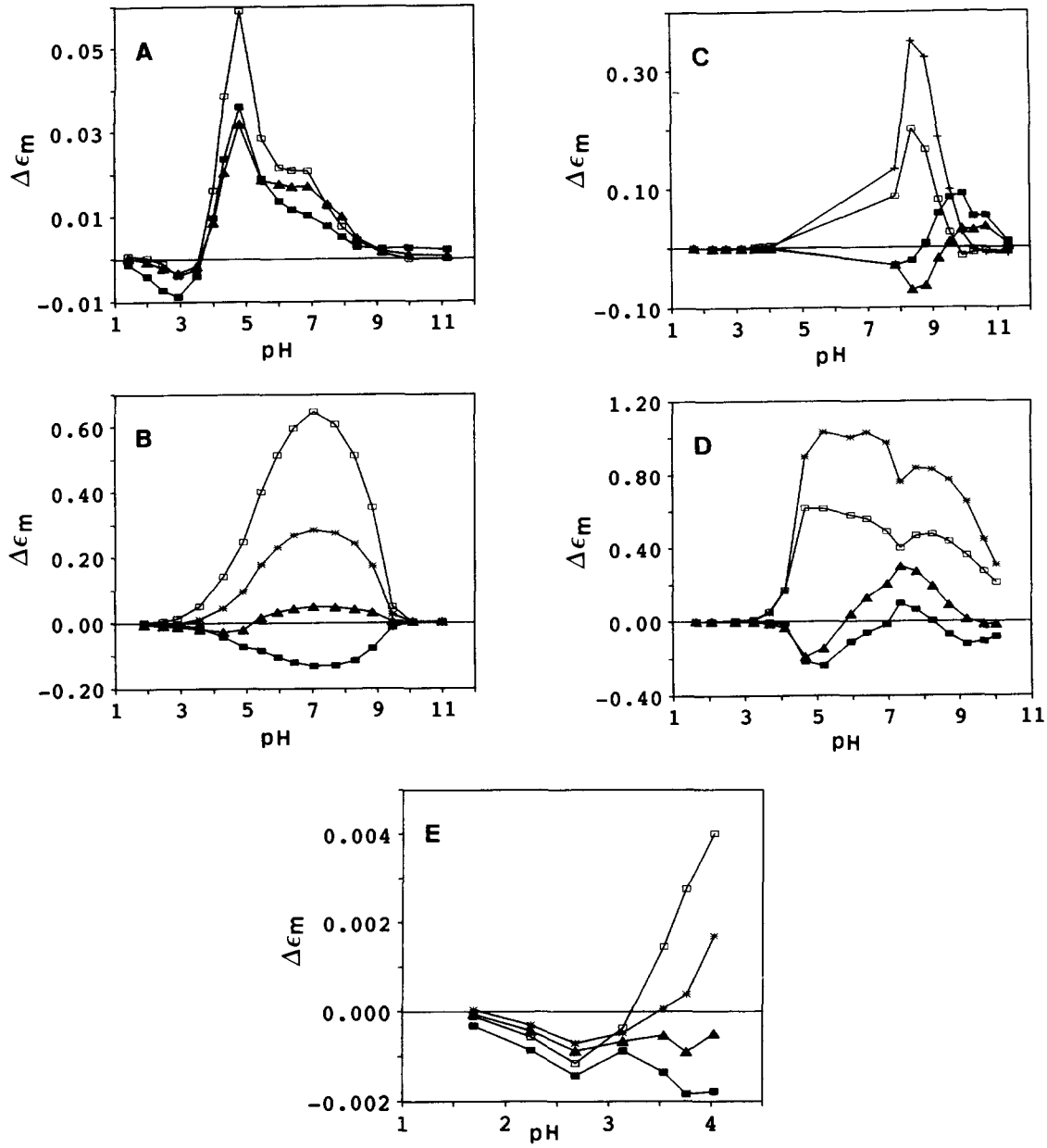


Fig. 14. Change with pH of the $\Delta\varepsilon_m$ values for solutions. (A) *N*α-Acetyl-L-histidine and $VO^{2+}$ with L/M = 10.0 and $C_{VO} = 0.012$–$0.008$ M. (■) 595 nm; (▲) 680 nm; (□) 775 nm. (B) 1-Methyl-L-histidine and $VO^{2+}$ with L/M = 15.0 and $C_{VO} = 0.012$–$0.011$ M. (□) 535 nm; (▲) 590 nm; (*) 650 nm; (■) 740 nm. (C) L-Histidinol and $VO^{2+}$ with L/M = 15.2 and $C_{VO} = 0.018$–$0.013$ M. (■) 530 nm; (▲) 590 nm; (□) 730 nm; (+) 830 nm. (D) L-Histidine methyl ester and $VO^{2+}$ with L/M = 20.0 and $C_{VO} = 0.015$–$0.008$ M. (■) 490 nm; (▲) 530 nm; (□) 690; (*) 750 nm. (E) L-Histidinol and $VO^{2+}$ with L/M = 15.2 and $C_{VO} \cong 0.018$ M. (■) 530 nm; (▲) 590 nm; (□) 730 nm; (+) 830 nm. Expanded scales of C for the low pH range.

11). However, oligomers are present in significant concentrations, as indicated by the brown colour of the solutions and the visible spectra (Fig. 10B).

Restricting our discussion to the monomeric species present, at pH ~ 8.4 the solution probably contains a mixture of VII* and IV*, possibly corresponding to structures **20** and **21**, respectively (whether VI* and VII* are distinct species is uncertain). For pH ≳ 8, the ESR signal (Fig. 7B) shifts to lower field values, but this may be due to the appearance of IV*. The pattern of the CD spectra changes as pH is increased from 8.3 to 9.9, an iso-

Table 2. Coordination geometries[a] and corresponding $A_{\parallel}$ estimated according to Chasteen's table,[9] assuming the contribution of $N_{im}$ is $162.8 \times 10^{-4}$ cm$^{-1}$

| Structure (schematic) | $A_{\parallel}$ ($\times 10^{+4}$ cm$^{-1}$) | Structure (schematic) | $A_{\parallel}$ ($\times 10^{+4}$ cm$^{-1}$) | Structure (schematic) | $A_{\parallel}$ ($\times 10^{+4}$ cm$^{-1}$) |
|---|---|---|---|---|---|
| 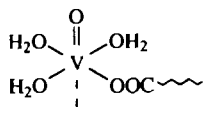 (8) | ~180 | 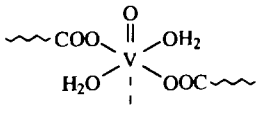 (9) | ~177 | 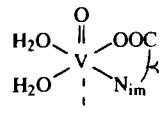 (10) | ~175 |
| 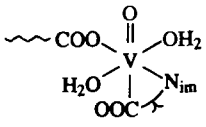 (11) | ~175 | 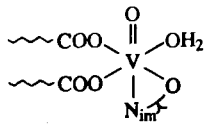 (12) | ~174 | 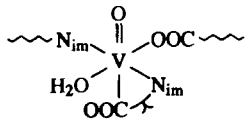 (13) | ~170 |
| 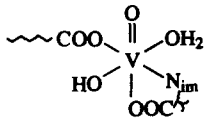 (14) | ~168 | 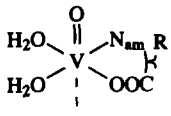 (15) | ~174 | 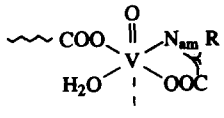 (16) | ~171 |
| 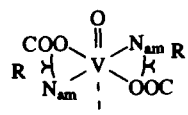 *cis* and/or *trans* (17) | ~166 | 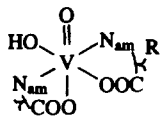 (18) | ~162 | 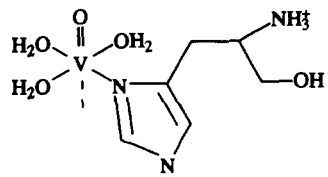 (19) | ~178 |
| 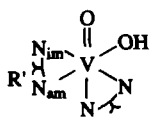 (20)[b] | ~160 | 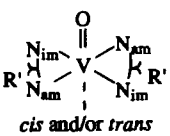 *cis* and/or *trans* (21) | ~162 | 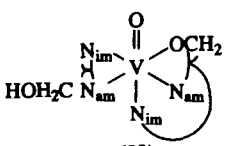 (22) | ~156 |
| 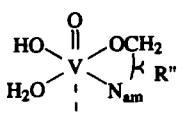 (23) | ~160 | 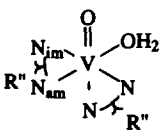 (24)[b] | ~167 | 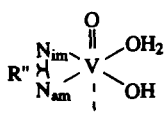 (25) | ~165 |

[a] For several of the structures included, other isomers are possible.

[b] As either $N_{am}$ or $N_{im}$ could be coordinated equatorial, they are not specified. $A_{\parallel}$ was estimated assuming $A_{\parallel}$ (N) = $161.5 \times 10^{-4}$ cm$^{-1}$.

dichroic point being detected at ~628 nm. These CD spectra suggest the existence of an equilibrium between (at least) two optically active complexes: VII* ( and VI* ?) and IX*. Species IX* is responsible for the positive $\Delta\varepsilon_m$ values in the range 450–620 nm at pH ~ 10. Its coordination geometry involves the equatorial coordination of the R—$O^-$ group of one histidinol ligand. Likely coordination geometries are e.g. **22** and **23**.

For pH > 10, there is a general decrease in the $|\Delta\varepsilon_m|$ values as pH is increased (Figs 11C and 14C), indicating further hydrolysis and gradual substitution of **5** by $OH^-$.

*Histidine methyl ester*

In the pH range 1.7–3.7, the estimated $g$ and $A$ ($\perp$ and $\|$) parameters for the main species detected (Fig. 7A and Table 1) suggest the formation of $[VO(OH_2)_5]^{2+}$, consistent with the very low $\Delta\varepsilon_m$ values (Figs 9A and 14D) and visible spectra (Fig. 8). The presence of a small amount of L-histidine in the starting material may account for the greater $\varepsilon_m$ values in the range 650–800 nm than for the L-histidinol or histamine + oxovanadium(IV) in similar conditions.

In the pH range 4.5–10, the spectra were recorded in the order specified in Figs 8 and 9. The high $\varepsilon_m$ values in the visible spectra (Fig. 8) indicate that a small amount of oligomeric species is present throughout this range. In the pH range 4.5–5.8, the CD spectra are like those for similar solutions containing L-his or 3Mehis + oxovanadium(IV), but the $|\Delta\varepsilon_m|$ values are ~20% lower. Species $IV^{\oplus}$ and $V^{\oplus}$ could correspond to coordination geometries such as **21** and **24**, respectively. This would mean that their concentration ratio is not pH dependent. If this is correct the changes in the relative intensities of the corresponding ESR peaks are due to the formation of $VI^{\oplus}$ and $VII^{\oplus}$, detected very close to $V^{\oplus}$.

In the pH range 6–9, the pattern of the CD spectra for band II changes (Figs 9B and 14D) and becomes quite different from those obtained for solutions containing L-his or 3Mehis + oxovanadium(IV) in similar conditions. This corresponds to the formation of species $VI^{\oplus}$ detected in the ESR. For pH > 9, the pattern of the CD spectra changes again and becomes similar to those for similar solutions containing L-his or 3Mehis + oxovanadium(IV). This now corresponds to the formation of species $VII^{\oplus}$ detected in the ESR.

Species $VI^{\oplus}$ could correspond to an equatorial $(N_{im})_2(N_{am})_2$ donor set and an $OH^-$ group axial. Species $VII^{\oplus}$ could correspond to structures such as **20**. However, this would probably have $A_{\|}$ values lower than for $IV^{\oplus}$,[9] contrary to observation. Structures such as **25** cannot be ruled out, but they would not explain the high $|\Delta\varepsilon_m|$ values for species $ML_2H_{-1}$ that forms in the L-his and 3Mehis + $VO^{2+}$ system and possibly corresponds to $VII^{\oplus}$.

*Histamine*

Up to pH ~ 4 the estimated $g$ and $A$ ($\perp$ and $\|$) parameters for the main species (Fig. 12 and Table 1) are consistent with the formation of $[VO(OH_2)_5]^{2+}$. Indeed, the $\varepsilon_m$ values of the visible spectra in the pH range 1.6–3.5 (Fig. 13) practically coincide with an oxovanadium(IV) solution.

The ESR spectrum at pH 3.89 (Fig. 12) is very similar to that at pH 3.76 for the histidinol + $VO^{2+}$ system (Fig. 7B). In particular, the species $I^{\#}$ in Fig. 12 probably corresponds to the same coordination geometry as I*. At pH ~ 3.9, the visible spectrum indicates partial hydrolysis of oxovanadium (IV) (i.e. $[(VO)_2(OH)_2]^{2+}$, which is ESR silent, forms in a relatively low concentration).

As with **5**, vanadyl hydroxide precipitates for pH > 4. If base is (rapidly) added before a significant amount of solid forms, for pH > 8 it dissolves to a brown solution. The ESR spectra differ from those for the other systems in this study, and a single species ($VII^{\#}$) is detected at pH 8.3. The ESR signal is much weaker than for the low pH region; oxovanadium(IV) is significantly hydrolysed to oligomeric species which are ESR silent (e.g. $\{[(VO)_2(OH)_5]^-\}_n$[14]). Species $VII^{\#}$ possibly corresponds to structure **21**; however, structures such as **20** are also plausible.

These results indicate that for L-his and 3Mehis + $VO^{2+}$ systems the coordination of the R—$COO^-$ group is important. Its absence, as with **5** or **7**, produces completely different spectroscopic results, and vanadyl hydroxide precipitation occurs even with L/M ratios as high as 20. For histamine, $pK_a(N_{im}H) = 6.07$ and $pK_a(N_{am}H) = 9.79$, compared to 6.03 and 9.09, respectively, for L-his in the same medium (25°C; $I = 0.1$ M).[17] Besides the absence of $COO^-$ donor group, the increase of 0.7 units in $pK_a(N_{am}H)$ for **7** also gives rise to lower availability for its coordination to $VO^{2+}$. The opposite effect occurs for **4**: its $pK_a(N_{am}H)$ is probably significantly lower than for L-his, and although $VO^{2+}$ hydrolyses appreciably for pH > 4, vanadyl hydroxide precipitation can be avoided.

## CONCLUSION

For most natural amino acids (from proteins), solutions with low L/M ratios contain much hydro-

lysed $VO^{2+}$. For the three amino acids L-histidine, L-cysteine and aspartic acid, it is possible to avoid this extensive $VO^{2+}$ hydrolysis. Of these, only for L-histidine has a $VO^{2+}$ α-amino acid complex been characterized by X-ray diffraction.[2]

Comparisons between the pH dependence of the visible CD, visible isotropic absorption and ESR spectra obtained earlier for the L-histidine + $VO^{2+}$ system[5] with those for several L-histidine derivatives and related ligands included in this present work clarify the coordination modes of the ligand L-histidine.

Among the conclusions, the tridentate coordination of one of the L-histidine ligands in the pH range 6–8 is clearly proven. In fact:

(a) Substitution on the amino nitrogen, as in *N*α-acetyl-L-histidine, gives rise to extensive $VO^{2+}$ hydrolysis and eventually precipitation.
(b) Blocking the imidazole nitrogen, as in 1-methyl-L-histidine, produces rather similar results.
(c) When the $COO^-$ group is modified, as in L-histidine methyl ester, L-histidinol and (especially) histamine, extensive $VO^{2+}$ hydrolysis occurs, but species containing the $(N_{im})_2$ $(N_{am})_2$ donor set are detected.
(d) The results obtained for 3-methyl-L-histidine + $VO^{2+}$ are almost identical to those for L-histidine.

*Acknowledgements*—We thank Fundação Calouste Gulbenkian, Fundo Europeu para o Desenvolvimento Regional (FEDER), Junta Nacional de Investigação Científica e Tecnológica (JNICT), and programs STRIDE (project ref. STRDA/C/CEN/436/92) and CIENCIA (BD 859/90-RM) for financial support and R. Duarte and J. J. G. Moura for the use of their ESR facilities. We also thank the University of Wales, Cardiff, for a grant of leave (R.D.G.).

## REFERENCES

1. V. Vergopoulos, W. Priebsch, M. Fritzche and D. Rieder, *Inorg. Chem.* 1993, **32**, 1844 and references therein.
2. L. Xiaoping and Z. Kangjing, *J. Cryst. Spectrosc. Res.* 1986, **16**, 681.
3. K. Kanamori, M. Teraoka, H. Maeda and K. Okamoto, *Chem. Lett.* 1993, 1731.
4. J. Costa Pessoa, S. M. Luz and R. D. Gillard, *J. Inorg. Biochem.* 1993, **51**, 156.
5. J. Costa Pessoa, S. M. Luz, I. Cavaco and R. D. Gillard, *Polyhedron* 1994, **13**, 3177.
6. J. Costa Pessoa, L. F. Vilas Boas, R. D. Gillard and R. J. Lancashire, *Polyhedron* 1988, **7**, 1245 (Part I).
7. E. D. Moffat and R. I. Lytle, *Analyt. Chem.* 1959, **31**, 926.
8. L. Casella, M. Gullotti and A. Pintar, *Inorg. Chim. Acta* 1988, **144**, 89.
9. N. D. Chasteen, in *Biological Magnetic Resonance* (Edited by J. Lawrence, L. J. Berliner and J. Reuben), Vol. 3, Ch. 2, pp. 79–84. Plenum Press, New York (1981).
10. J. Costa Pessoa, S. M. Luz and R. D. Gillard, *Polyhedron* 1993, **12**, 2857.
11. E. W. Wilson Jr, M. H. Kasperian and R. B. Martin, *J. Am. Chem. Soc.* 1970, **92**, 5365.
12. L. Casella and M. Gullotti, *J. Inorg. Biochem.* 1983, **18**, 19 and references therein.
13. L. Casella and M. Gullotti, *Inorg. Chem.* 1983, **22**, 242.
14. L. F. Vilas Boas and J. Costa Pessoa, Chapter on Vanadium, in *Comprehensive Coordination Chemistry* (Edited by G. Wilkinson, R. D. Gillard and J. A. McCleverty), Vol. 3, pp. 453–583. Pergamon Press, Oxford (1987) and references therein.
15. J. Costa Pessoa, L. F. Vilas Boas and R. D. Gillard, *Polyhedron* 1989, **8**, 1173 (Part II).
16. A. Dessi, G. Micera and D. Sanna, *J. Inorg. Biochem.* 1993, **52**, 275.
17. G. Arena, R. Cali, V. Cucinotta, S. Musumeci, E. Rizzarelli and S. Sammartano, *J. Chem. Soc., Dalton Trans.* 1984, 1651.